Abdominal Radiology

Published online: 23 August 2018

Abdom Radiol (2019) 44:239–246
https://doi.org/10.1007/s00261-018-1728-4

High signal renal tumors on DWI: the diagnostic value of morphological characteristics

Hongtao Zhang,[1,2] Jingjing Pan,[1,3] Yanguang Shen,[1] Xu Bai,[1] Yingwei Wang,[1] Haiyi Wang,[1] and Huiyi Ye[1]

[1]Department of Radiology, Chinese PLA General Hospital, Fuxing Road 28, Beijing 100853, China
[2]Department of Radiology, 307 Hospital, PLA, Beijing, China
[3]Department of Radiology, General Hospital of the PLA Rocket Force, Beijing, China

Abstract

Purpose: To assess the usefulness of morphological characteristics of diffusion-weighted imaging (DWI) for differentiating malignant renal tumors from benign renal tumors, and clear cell renal cell carcinoma (RCC) from non-clear cell RCC at 3.0 T.
Methods: The study included 249 patients with 251 histopathologically confirmed renal tumors that showed high signal on DWI. For each tumor, two radiologists independently evaluated apparent diffusion coefficient (ADC) values and morphological characteristics of DWI. The differences in the quantitative and qualitative magnetic resonance imaging (MRI) features determined by the readers were assessed. The ADC values between malignant and benign renal tumors and between clear cell and non-clear cell RCC were compared using Mann–Whitney tests. The proportional differences of morphological characteristics of DWI between malignant and benign renal tumors and between clear cell and non-clear cell RCC were compared using Chi-square tests.
Results: There were no significant differences in the quantitative and qualitative MRI features determined by the readers. The ADC values for malignant renal tumors were statistically significantly higher than those for benign renal tumors ($p < 0.05$), and the ADC values for clear cell RCC were statistically significantly higher than those for non-clear cell RCC ($p < 0.05$). The proportion of morphological characteristics of DWI between malignant and benign renal tumors was statistically significantly different at ring, nodular, flaky high signal. The proportion of morphological characteristics of DWI between clear cell and non-clear cell RCC was statistically significantly different at uniform high signal.
Conclusions: The morphological characteristics of DWI are useful in differentiating renal tumors.

Key words: Renal tumors—Diffusion-weighted imaging, DWI—Magnetic resonance imaging, MRI—Morphological characteristics

The incidence of renal cell carcinoma (RCC) has increased in recent years [1]. This increase is partly attributed to the more widespread use of imaging and the resulting increase in the detection of small (≤ 4 cm) mostly asymptomatic lesions [2]. RCC has different histopathologic subtypes, which differ not only in their genomic profiles but also in their metastatic potential and outcomes [3]. Clear cell RCC, for example, accounts for the vast majority of all metastatic tumors and is associated with a worse outcome than RCC subtypes such as papillary or chromophobe RCC, which are more indolent [4, 5].

The understanding that nearly half of all patients with diagnosed renal cortical tumors will prove to have disease of a benign or indolent subtype has provided an incentive for the use of more conservative treatment approaches, with kidney-sparing resection performed whenever possible. A strong clinical need has developed for new imaging techniques that can help characterize renal cortical lesions preoperatively [6]. Over the last decade, MRI protocols for renal mass evaluation have evolved to include diffusion-weighted imaging (DWI) [7]. DWI captures inherent differences in how tissues restrict water motion for use in qualitative and quantitative evaluations based on the apparent diffusion coefficient (ADC) [8]. DWI has thus been investigated as a supplement to conventional MRI sequences [9–11]. The studies in the literature on DWI performance for renal

Hongtao Zhang and Jingjing Pan have contributed equally to this study.

Correspondence to: Haiyi Wang; *email:* wanghaiyi301@126.com; Huiyi Ye; *email:* 13701100368@163.com

mass characterization include DWI-based discrimination between malignant and benign renal lesions, differentiation among RCC subtypes, and differentiation of high- from low-grade clear cell RCCs [12–14]. The previous studies have been focused on the role of quantitative evaluation of ADC values. The morphological characteristics of DWI have not been widely studied.

The purpose of this study was therefore to investigate the usefulness of morphological characteristics of DWI for differentiating malignant renal tumors from benign renal tumors, and clear cell RCC from non-clear cell RCC at 3.0 T.

Materials and methods

Patients

Our Institutional Review Board approved this retrospective study, and the need to obtain informed consent was waived. All methods were performed in accordance with the approved guidelines. A retrospective review was performed of all patients from January 2016 to February 2017 who underwent MR imaging for evaluation of renal masses and who had pathologic confirmation of the renal masses. Of the 533 patients who had undergone MRI between January 2016 and February 2017, 249 were included in our study.

The inclusion criteria were as follows: (1) patients had to have undergone an MRI examination with a standardized renal multiparametric MRI (mpMRI) protocol at 3.0 T, including a DW sequence; (2) all renal masses showed high signal on DWI compared with the renal cortex; (3) all renal masses had surgical pathology or percutaneous renal biopsy pathology; and (4) all the examinations were performed before surgery or percutaneous renal biopsy. The exclusion criteria were as follows: (1) DW images were affected by heavy distortion and 8 patients were excluded; and (2) renal masses showed hypo- or isointensity on DWI.

MR imaging protocol

MR imaging examinations were performed with a 3.0-T system (Signa EXCITE; GE Healthcare) and a 3.0-T system (Discovery 750, GE Healthcare). Patients were imaged in the supine position using a surface phased-array coil. Respiratory-triggered transverse and coronal T2-weighted fast spin-echo sequences were initially performed, and this was followed by transverse T1-weighted dual-echo in-phase and out-of-phase sequences and by three-dimensional fat-saturated T1-weighted dynamic contrast-enhanced sequences that were performed during suspended respiration. Gadobenate dimeglumine (MultiHance; Bracco Sine, Shanghai, China) (15 mL) was injected intravenously at a rate of 2 mL/sec using a power injector (Spectris; MedRad, Warrendale, PA), and this was followed by a 20-mL saline flush. Dynamic contrast-enhanced MR imaging was performed in the transverse plane at baseline (pre-contrast), during the arterial phase, and 30 and 240 s after the arterial phase. Transverse breath-hold DW images were obtained using a single-shot, spin-echo echo-planar sequence before the administration of contrast material with tridirectional gradients and two b values: 0 and 800 s/mm^2.

The MR imaging parameters were as follows: T2-w FSE images were acquired using the following parameters: infinite/90–105 ms (repetition time ms/echo time ms); field of view (FOV), 36–40 cm; section thickness, 5 mm; intersection gap, 1 mm; and matrix, 320 × 224. T1-w dual-echo images were acquired using the following parameters: 260/(2.2–2.5; 5.5–5.8) ms; FOV, 36–40 cm; section thickness, 5 mm; intersection gap, 1 mm; and matrix, 256 × 192. For the 3D dynamic contrast-enhanced sequences, the following parameters were used: 3.0–3.9/1.2–1.6 ms; FOV, 34–40 cm; section thickness, 5 mm; interpolated section thickness, 2.5 mm; and matrix, 288 × 224.DWI (5400/50–60 ms; flip angle, 90°; FOV, 36–40 cm; matrix, 128 × 128; section thickness, 5 mm; intersection gap, 1 mm; all directions; one signal acquired) was performed before the dynamic contrast-enhanced MRI (DCE-MRI) with *b* values of 0 and 800 s/mm^2.

Image analysis

All images were independently reviewed by two radiologists who had 10 and 5 years of experience in the interpretation of abdominal MR images. The two reviewers were blinded to the histopathologic diagnoses of the lesions at the time of their review. The final decisions were reached by consensus.

ADC values

ADC maps were autogenerated, and region-of-interest (ROI) analysis was performed using an Advantage Workstation (Advantage Workstation, version 4.6, GE Healthcare, Bue, France). ROIs were placed within the tumor on DW images. The intratumoral ROI was placed at a single location within the region of the tumor seen to be brightest on the basis of visual assessment, avoiding regions of necrosis, hemorrhage, and cystic degeneration, which typically show no enhancement on dynamic contrast-enhanced MR images. For each reader, the tumor was measured three times, and the mean ADC values were calculated for each tumor, each measuring 30–60 mm^2. The mean values for the two readers were regarded as the final ADC value.

Morphological characteristics on DWI

The shape of the high signal was divided into ring (ring high signal is defined as the peripheral part of the lesion being high signal and the center part being low signal),

nodular, flaky (flaky high signal is defined as noncircular or nonnodular lesion and the ratio of length to width being greater than two), and uniform high signal. The signal intensity was compared to that of normal renal cortex on DWI and assessed to be higher, lower, or equivalent to that of normal renal cortex.

Pathologic diagnosis

The reference standard for the final diagnosis was the histopathologic result in the specimen obtained at surgical resection or puncture biopsy in all patients. All specimens were retrospectively examined by two uropathologists with 10 years of experience in uropathology who were blinded to the MRI findings and who reached consensus.

Statistical analysis

Continuous variables were expressed as the mean ± SD and were analyzed using independent *t* tests for normally distributed data or Mann–Whitney tests for nonnormally distributed data. For qualitative variables, Chi-square tests were used to compare the sample proportion of the two readers. Kappa coefficients were not used for this determination because the very high prevalence of certain imaging features for many of the binary factors was expected to produce misleadingly low values. All reported *P* values are two sided and were considered statistically significant at values of less than 0.05. SPSS version 22.0 software was used for all computations.

Results

Patient and tumor characteristics

A total of 249 patients (mean age, 52.8 years; range 10–86 years) with 251 renal cortical lesions were included in the study. 166 of the patients (67%) were men (mean age, 53.3 years; age range 15–86 years), and 83(33%) were women (mean age, 51.7 years; age range 10–75 years). On the basis of findings from histopathologic evaluation, 16 of the 251 tumors (6.3%) were characterized as angiomyolipoma (13 tumors were classic AMLs and 3 were fat-poor AMLs), 5 (2%) as PEComa, 2 (0.8%) as hemangioma,1 (0.4%) as oncocytoma, 1 (0.4%) as leiomyoma,1 (0.4%) as schwannoma,186 (74.1%) as clear cell RCC, 14 (5.6%) as papillary RCC,9 (3.6%) as chromophobe RCC, 5 (2%) as renal carcinoma associated with Xp11.2 translocations/TFE3 gene fusions, 2 (0.8%) as Wilms' tumor, 2 (0.8%) as mucinous tubular spindle cell carcinoma, 2 (0.8%) as neuroendocrine carcinoma, 2 (0.8%) as PNET, 1 (0.4%) as sarcomatoid carcinoma, 2(0.8%) as unclassified RCC. Mean tumor size was 52.4 mm (range 12–217 mm). Patient characteristics are summarized in Table 1. When we discussed nonclear cell RCC, only papillary and chromophobic RCCs were included, because papillary and chromophobic RCCs are more common in non-clear cell RCC and in clinical work.

ADC values

ADC values are summarized in Table 2. There were no significant differences between the assessments made by the two readers. For final results, ADC values for malignant renal tumors were statistically significantly higher than those for benign renal tumors ($p < 0.05$), and ADC values for clear cell RCC were statistically significantly higher than those for non-clear cell RCC ($p < 0.05$).

Morphological characteristics

A renal tumor may have one or two morphological features on DWI, but no lesion had three or four morphological features.

No statistically significant differences were recorded between the two readers in proportion of assessed morphological characteristics of DWI in renal tumors (Table 3).

For final results, the proportion of morphological characteristics of DWI between malignant and benign renal tumors was statistically significantly different at ring, nodular, flaky high signal morphological characteristics (Table 4). The proportion of ring and nodular high signal morphological characteristics is high in malignant renal tumors (Figs. 1, 2). The proportion of flaky high signal morphological characteristics is high in benign renal tumors (Figs. 3). The proportion of morphological characteristics of DWI between clear cell and non-clear cell RCC was statistically significantly different at uniform high signal morphological characteristics (Table 4). The proportion of uniform high signal morphological characteristics is high in non-clear cell RCC (Figs. 4).

Discussion

DWI is of particular value for characterizing renal tumors [15–17], because it allows visualization and quantification of cell density, the integrity of cell membranes, and tissue architecture, and because its ability to assess the tumor microenvironment has already been proven to be of value in other areas of oncologic imaging [18, 19]. The previous results provided an estimate of the accuracy of DWI for distinguishing malignant from benign renal masses with a sensitivity of 86% and specificity of 78% [20]. Furthermore, no application of contrast agent is necessary for its acquisition, which is an additional benefit for patients with impaired renal function. Therefore, the role of DWI in the diagnosis and differ-

Table 1. Patient demographics and clinical characteristics

Characteristics	Malignant tumors	Benign tumors	*P* value
Age (years)	53.7 ± 13.2	45.1 ± 11.7	< 0.05
male/female (*n*)	157/66	9/17	< 0.05
Diameter (mm)	51.1 ± 25.6	64 ± 53.9	> 0.05
	Clear cell RCC	Nonclear cell RCC	
Age (years)	55.4 ± 11.5	51.6 ± 15.7	> 0.05
male/female (*n*)	136/49	14/8	> 0.05
Diameter (mm)	52.4 ± 26.1	42.3 ± 23.9	> 0.05

(*n*) is numbers of patients. Other data are mean values ± standard deviations

Table 2. ADC values of renal tumors

Classification	Reader 1	Reader 2	*P* value
Malignant tumors	1.11 ± 0.24	1.17 ± 0.22	> 0.05
Benign tumors	1.01 ± 0.21	1.09 ± 0.19	> 0.05
Clear cell RCC	1.16 ± 0.21	1.14 ± 0.22	> 0.05
Nonclear cell RCC	0.86 ± 0.22	0.78 ± 0.19	> 0.05
	Malignant tumors	Benign tumors	*P* value
ADC value	1.14 ± 0.23	1.02 ± 0.21	< 0.05
	Clear cell RCC	Nonclear cell RCC	
ADC value	1.15 ± 0.22	0.82 ± 0.21	< 0.05

Values are mean values ± standard deviations. ADCs are expressed as $\times 10^{-3}$ mm^2/sec

Table 3. Frequency of assessed morphological characteristics of DWI in renal tumors for the two readers

Classification	Characteristics	Reader 1	Reader 2	*P* value
Malignant tumors	Ring high signal	39.6 (89/225)	40.9 (92/225)	0.773
	Nodular high signal	54.7 (123/225)	53.3 (120/225)	0.85
	Flaky high signal	13.8 (31/225)	12.4 (28/225)	0.675
	uniform high signal	8 (18/225)	8 (18/225)	1
Benign tumors	Ring high signal	3.8 (1/26)	7.7 (2/26)	0.548
	Nodular high signal	7.7 (2/26)	11.5 (3/26)	0.638
	Flaky high signal	84.6 (22/26)	92.3 (24/26)	0.385
	uniform high signal	15.4 (4/26)	15.4 (4/26)	1
Clear cell RCC	Ring high signal	42.5 (79/186)	45.2 (84/186)	0.601
	Nodular high signal	55.4 (103/186)	54.3 (101/186)	0.835
	Flaky high signal	13.4 (25/186)	14.5 (27/186)	0.765
	uniform high signal	2.7(5/186)	2.7 (5/186)	1
Nonclear cell RCC	Ring high signal	30.4 (7/23)	26.1 (6/23)	0.743
	Nodular high signal	39.1 (9/23)	47.8 (11/23)	0.552
	Flaky high signal	17.4(4/23)	21.7 (5/23)	0.710
	uniform high signal	30.4 (7/23)	30.4 (7/23)	1

Data are percentages with raw numbers of patients (*n*) in parenthesis. *P* values were calculated using χ^2 tests

ential diagnosis of renal masses has become more and more important [21–23].

In our study, the ADC values for malignant renal masses were statistically significantly higher than those for benign renal masses. One reason was that the results have been obtained in a group of hyperintense DWI lesions. The other one was that clear cell RCC accounted for a large proportion of malignant renal tumors in our cases (82.7%), the number of benign renal tumors was relatively small, accounting for 10.4% of all lesions, and the number of angiomyolipomas was high in benign renal tumors. The ADC values for clear cell RCC were

Table 4. Frequency of assessed morphological characteristics of DWI in renal tumors by consensus

Characteristics	Malignant tumors	Benign tumors	*P* Value
Ring high signal	40 (90/225)	3.8 (1/26)	< 0.05
Nodular high signal	54.2 (122/225)	7.7 (2/26)	< 0.05
Flaky high signal	14.2 (32/225)	88.5 (23/26)	< 0.05
uniform high signal	8 (18/225)	15.4 (4/26)	0.371
	Clear cell RCC	Nonclear cell RCC	
Ring high signal	43 (80/186)	30.4 (7/23)	0.248
Nodular high signal	55.9 (104/186)	43.5 (10/23)	0.259
Flaky high signal	13.4 (25/186)	17.4 (4/23)	0.844
uniform high signal	2.7 (5/186)	30.4 (7/23)	< 0.05

Data are percentages with raw numbers of patients (*n*) in parenthesis. *P* values were calculated using $\chi 2$ tests

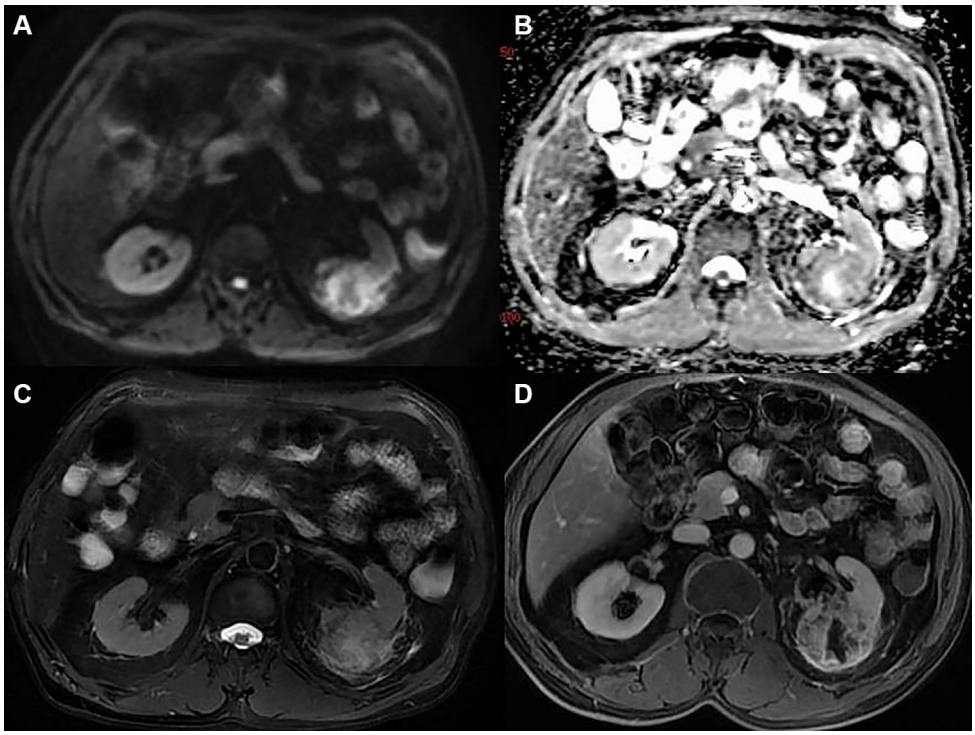

Fig. 1. Images in 70-year-old man with clear cell RCC in the lower pole of left kidney. **A** On axial DWI, the tumor shows ring high signal morphological characteristics. **B** On axial ADC map, the tumor shows ring low signal morphological characteristics. **C** On axial T2WI, the tumor shows slight hyperintensity on peripheral part and hyperintensity on central part compared with the normal renal parenchyma. **D** On contrast T1WI during the delayed phase, the tumor shows ring enhancement on peripheral part and necrosis on central part.

statistically significantly higher than those for non-clear cell RCC, consistent with results from previous reports. The underlying biologic causes for higher ADC values in clear cell RCC than in non-clear cell RCC remain unclear. It could be hypothesized that strongly increased blood perfusion and intratumoral angiogenesis, as found in clear cell RCC [24], could contribute to the high ADC values in clear cell RCC. This hypothesis is supported by the results of preliminary studies [25, 26] that used intravoxel incoherent motion imaging to assess tumor perfusion and also reported higher values for perfusion parameters in clear cell RCC.

Through our investigation, the proportion of morphological characteristics of DWI between malignant and benign renal tumors was statistically significantly different at ring, nodular, flaky signal morphological characteristics. The proportion of ring and nodular signal morphological characteristics was high in malignant renal tumors. These two kinds of morphological characteristics of DWI reflect the growth characteristics of

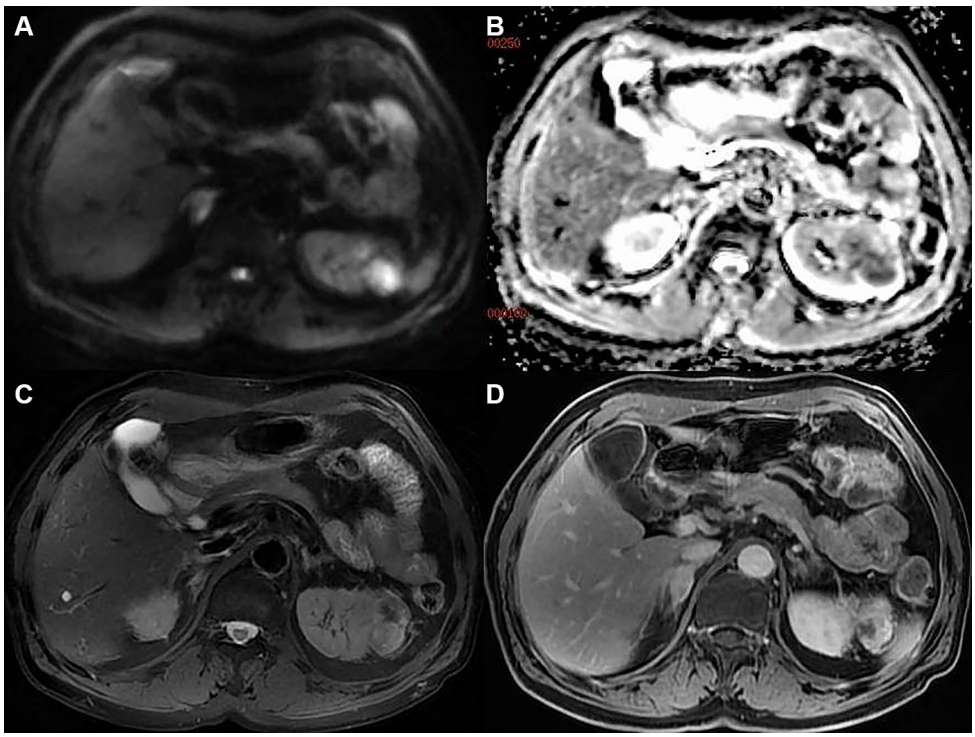

Fig. 2. Images in 73-year-old man with clear cell RCC in the upper pole of left kidney. **A** On axial DWI, the tumor shows nodular high signal morphological characteristics on peripheral part. **B** On axial ADC map, the tumor shows nodular low signal morphological characteristics on peripheral part. **C** On axial T2WI, the tumor shows slightly heterogeneous hyperintensity. **D** On contrast T1WI during the delayed phase, the nodule shows obvious enhancement.

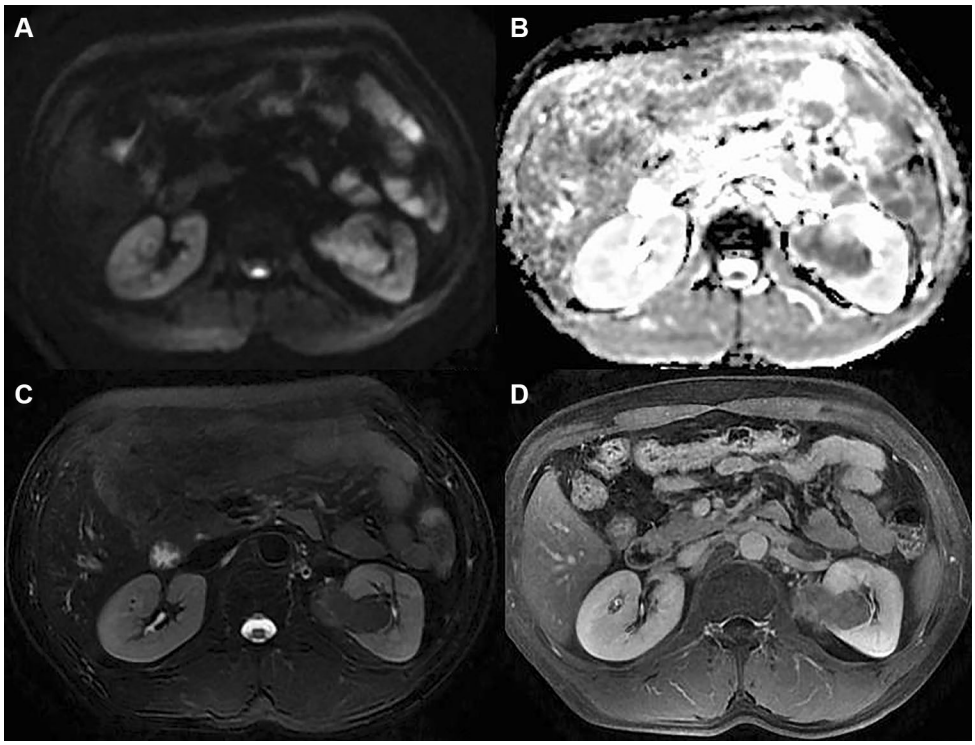

Fig. 3. Images in 28-year-old man with angiomyolipoma in the upper pole of left kidney. **A** On axial DWI, the tumor shows flaky high signal morphological characteristics. **B** On axial ADC map, the tumor shows flaky low signal morphological characteristics. **C** On axial T2WI, the tumor shows homogeneous hypointensity. **D** On contrast T1WI during the delayed phase, the tumor shows slight enhancement.

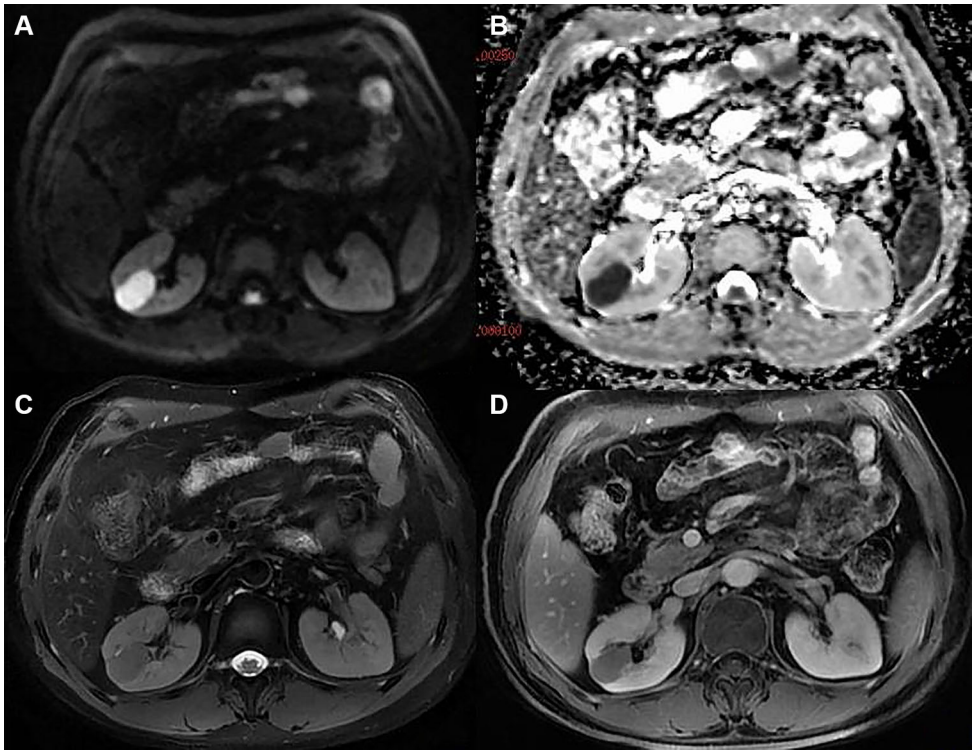

Fig. 4. Images in 47-year-old man with papillary RCC in the midportion of right kidney. **A** On axial DWI, the tumor shows uniform high signal morphological characteristics. **B** On axial ADC map, the tumor shows uniform low signal morphological characteristics. **C** On axial T2WI, the tumor shows slightly homogeneous hypointensity. **D** On contrast T1WI during the delayed phase, the tumor shows slight enhancement.

malignant tumors [27]. The growth of the tumor cells is active, and the density of the tumor cells is dense in the peripheral part of the malignant tumors, so the peripheral part shows hyperintensity on DWI. The growth of the tumor cells is inactive or tumor necrosis is formed on the central part of the malignant tumors, so the center part shows hypointensity on DWI. In malignant tumors, the growth rate of the tumor cells on different parts of the lesion is different, and the growth of the tumor cells is active, and the density of the tumor cells is dense in local part of the malignant tumors [28, 29]. Therefore, the local part of the malignant tumors shows hyperintensity on DWI. Therefore, the ring and nodular high signal morphological characteristics provide valuable information for the diagnosis of malignant renal tumors. The proportion of flaky signal morphological characteristics is high in benign renal tumors. Therefore, the flaky high signal morphological characteristics provide valuable information for the diagnosis of benign renal tumors.

The usefulness of morphological characteristics of DWI for differentiating clear cell RCC from non-clear cell RCC at 3.0 T was also investigated in our study. The current studies in the literature has not provided a reliable estimate of the accuracy of DWI for the differentiation of clear cell RCC from non–clear cell RCC given that there is substantial heterogeneity among the few available studies [23, 30]. However, in our study, the proportion of morphological characteristics of DWI between clear cell and non-clear cell RCC was statistically significantly different at uniform high signal morphological characteristics. The proportion of uniform high signal morphological characteristics is high-in non-clear cell RCC. Therefore, the uniform high signal morphological characteristics provide valuable information for the diagnosis of non-clear cell RCC.

Our study had a number of limitations. First, this was a retrospective study with a relatively small sample size for non-clear cell RCC and benign renal tumors. Therefore, our findings regarding the differentiation of renal tumors will need to be validated by larger, ideally prospective, studies. Second, the images reviewed were obtained using different MR instruments; however, the same imaging protocols were used. Finally, because our study focused on the efficacy of DW imaging, the usefulness of other MRI sequences on differentiation of renal masses was not evaluated.

In conclusion, the morphological characteristics of DWI are useful in differentiating renal tumors, which is obtained in tumors with hyperintensity in DWI. The ring and nodular high signal morphological characteristics are useful in diagnosing malignant renal masses. The flaky high signal morphological characteristics are useful in diagnosing benign renal masses. The uniform high signal morphological characteristics are useful in diag-

nosing non-clear cell RCC. This finding could provide additional diagnostic information to help differentiate malignant renal tumors from benign renal tumors and clear cell RCC from non-clear cell RCC.

Compliance with ethical standards

Funding This study was supported by National Natural Science Foundation of China (No. 81771785 and 81471641). The funders had no role in research design, data collection, and analysis, decision to publish, or preparation of the manuscript.

Conflict of interest The authors declare that they have no conflict of interest.

Ethical approval All procedures performed in studies involving human participants were in accordance with the ethical standards of the institutional and/or national research committee and with the 1964 Helsinki declaration and its later amendments or comparable ethical standards.

References

1. Sun M, Thuret R, Abdollah F, et al. (2011) Age-adjusted incidence, mortality, and survival rates of stage-specific renal cell carcinoma in North America: a trend analysis. Eur Urol 59(1):135–141. https://doi.org/10.1016/j.eururo.2010.10.029
2. Hollingsworth JM, Miller DC, Daignault S, et al. (2006) Rising incidence of small renal masses:a need to reassess treatment effect. J Natl Cancer Inst 98(18):1331–1334. https://doi.org/10.1093/jnci/djj362
3. Cornelis F, Tricaud E, Lasserre AS, et al. (2014) Routinely performed multiparametric magnetic resonance imaging helps to differentiate common subtypes of renal tumours. Eur Radiol 24(5):1068–1080. https://doi.org/10.1007/s00330-014-3107-z
4. Beck SD, Patel MI, Snyder ME, et al. (2004) Effect of papillary and chromophobe cell type on disease-free survival after nephrectomy for renal cell carcinoma. Ann Surg Oncol 11(1):71–77
5. Leibovich BC, Lohse CM, Crispen PL, et al. (2010) Histological subtype is an independent predictor of outcome for patients with renal cell carcinoma. J Urol 183(4):1309–1315. https://doi.org/10.1016/j.juro.2009.12.035
6. Zhang J, Tehrani YM, Wang L, et al. (2008) Renal masses: characterization with diffusion-weighted MR imaging-a preliminary experience. Radiology 247(2):458–464. https://doi.org/10.1148/radiol.2472070823
7. Taouli B, Thakur RK, Mannelli L, et al. (2009) Renal lesions: characterization with diffusion-weighted imaging versus contrast-enhanced MR imaging. Radiology 251(2):398–407. https://doi.org/10.1148/radiol.2512080880
8. Ginat DT, Mangla R, Yeaney G, et al. (2012) Diffusion-weighted imaging for differentiating benign from malignant skull lesions and correlation with cell density. AJR Am J Roentgenol 198(6):W597–W601. https://doi.org/10.2214/AJR.11.7424
9. Kim S, Jain M, Harris AB, et al. (2009) T1 hyperintense renal lesions: characterization with diffusion-weighted MR imaging versus contrast-enhanced MR imaging. Radiology 251(3):796–807. https://doi.org/10.1148/radiol.2513080724
10. Sandrasegaran K, Sundaram CP, Ramaswamy R, et al. (2010) Usefulness of diffusion-weighted imaging in the evaluation of renal masses. AJR Am J Roentqenol 194(2):438–445. https://doi.org/10.2214/AJR.09.3024
11. Wang H, Cheng L, Zhang X, et al. (2010) Renal cell carcinoma: diffusion-weighted MR imaging for subtype differentiation at 3.0 T. Radiology 257(1):135–143. https://doi.org/10.1148/radiol.10092396
12. Yu X, Lin M, Ouyang H, et al. (2012) Application of ADC measurement in a characterization of renal cell carcinomas with different pathological types and grades by 3.0T diffusion weighted MRI. Eur J Radiol 81(11):3061–3066. https://doi.org/10.1016/j.ejrad.2012.04.028
13. Cornelis F, Tricaud E, Lasserre AS, et al. (2015) Multiparametric magnetic resonance imaging for the differentiation of low and high grade clear cell renal carcinoma. European radiology 25(1):24–31. https://doi.org/10.1007/s00330-014-3380-x
14. Sevcenco S, Heinz-Peer G, Ponhold L, et al. (2014) Utility and limitations of 3-Tesla diffusion-weighted magnetic resonance imaging for differentiation of renal tumors. Eur J Radiol 83(6):909–913. https://doi.org/10.1016/j.ejrad.2014.02.026
15. Razek AA, Farouk A, Mousa A, et al. (2011) Role of diffusion-weighted magnetic resonance imaging in characterization of renal tumors. J Comput Assist Tomogr 35(3):332–336. https://doi.org/10.1097/RCT.0b013e318219fe76
16. Lassel EA, Rao R, Schwenke C, et al. (2014) Diffusion-weighted imaging of focal renal lesions: a meta-analysis. Eur Radiol 24(1):241–249. https://doi.org/10.1007/s00330-013-3004-x
17. Goya C, Hamidi C, Bozkurt Y, et al. (2015) The role of apparent diffusion coefficient quantification in differentiating benign and malignant renal masses by 3 Tesla magnetic resonance imaging. Balkan Med J 32(3):273–278. https://doi.org/10.5152/balkanmedj.2015.15475
18. Inci E, Hocaoglu E, Aydin S, et al. (2012) Diffusion-weighted magnetic resonance imaging in evaluation of primary solid and cystic renal masses using the Bosniak classification. Eur J Radiol 81(5):815–820. https://doi.org/10.1016/j.ejrad.2011.02.024
19. Mirka H, Korcakova E, Kastner J, et al. (2015) Diffusion-weighted imaging using 3.0 T MRI as a possible biomarker of renal tumors. Anticancer Res 35(4):2351–2357
20. Kang SK, Zhang A, Pandharipande PV, et al. (2015) DWI for renal mass characterization: systematic review and meta-analysis of diagnostic test performance. AJR Am J Roentgenol 205(2):317–324. https://doi.org/10.2214/AJR.14.13930
21. Lei Y, Wang H, Li HF, et al. (2015) Diagnostic significance of diffusion weighted MRI in renal cancer. Biomed Res Int 2015:172165. https://doi.org/10.1155/2015/172165
22. Mirka H, Korcakova E, Kastner J, et al. (2015) Diffusion-weighted imaging using 3.0 T MRI as a possible biomarker of renal tumors. Anticancer Res 35(4):2351–2357
23. Hotker AM, Mazaheri Y, Wibmer A, et al. (2016) Use of DWI in the differentiation of renal cortical tumors. AJR Am J Roentgenol 206(1):100–105. https://doi.org/10.2214/AJR.14.13923
24. Aziz SA, Sznol J, Adeniran A, et al. (2013) Vascularity of primary and metastatic renal cell carcinoma specimens. J Transl Med 11:15. https://doi.org/10.1186/1479-5876-11-15
25. Rheinheimer S, Stieltjes B, Schneider F, et al. (2012) Investigation of renal lesions by diffusion-weighted magnetic resonance imaging applying intravoxel incoherent motion-derived parameters: initial experience. Eur J Radiol 81(3):e310–e316. https://doi.org/10.1016/j.ejrad.2011.10.016
26. Chandarana H, Kang SK, Wong S, et al. (2012) Diffusion-weighted intravoxel incoherent motion imaging of renal tumors with histopathologic correlation. Invest Radiol 47(12):688–696. https://doi.org/10.1097/RLI.0b013e31826a0a49
27. Thoeny HC, De Keyzer F (2007) Extracranial applications of diffusion-weighted magnetic resonance imaging. Eur Radiol 17(6):1385–1393. https://doi.org/10.1007/s00330-006-0547-0
28. Goyal A, Sharma R, Bhalla AS, et al. (2012) Diffusion-weighted MRI in renal cell carcinoma: A surrogate marker for predicting nuclear grade and histological subtype. Acta Radiol 53(3):349–358. https://doi.org/10.1258/ar.2011.110415
29. Tanaka H, Yoshida S, Fujii Y, et al. (2011) Diffusion-weighted magnetic resonance imaging in the differentiation of angiomyolipoma with minimal fat from clear cell renal cell carcinoma. Int J Urol 18(10):727–730. https://doi.org/10.1111/j.1442-2042.2011.02824.x
30. Kim SH, Kim CS, Kim MJ, et al. (2016) Differentiation of clear cell renal cell carcinoma from other subtypes and fat-poor angiomyolipoma by use of quantitative enhancement measurement during three-phase MDCT. AJR Am J Roentgenol 206(1):W21–W28. https://doi.org/10.2214/AJR.15.14666